

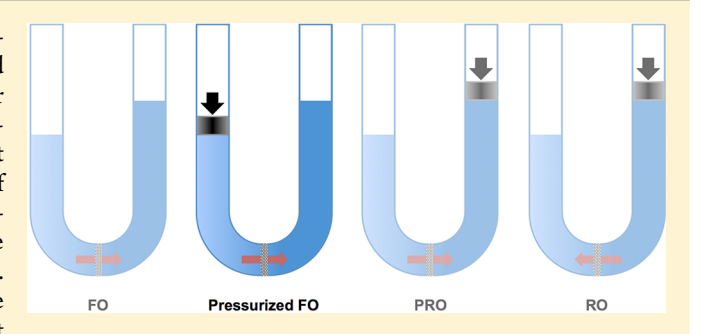


Effects of Transmembrane Hydraulic Pressure on Performance of **Forward Osmosis Membranes**

Bryan D. Coday, Dean M. Heil, Pei Xu, and Tzahi Y. Cath, and Tzahi Y. Cath

Supporting Information

ABSTRACT: Forward osmosis (FO) is an emerging membrane separation process that continues to be tested and implemented in various industrial water and wastewater treatment applications. The growing interests in the technology have prompted laboratories and manufacturers to adopt standard testing methods to ensure accurate comparison of membrane performance under laboratory-controlled conditions; however, standardized methods might not capture specific operating conditions unique to industrial applications. Experiments with cellulose triacetate (CTA) and polyamide thin-film composite (TFC) FO membranes demonstrated that



hydraulic transmembrane pressure (TMP), common in industrial operation of FO membrane elements, could affect membrane performance. Experiments were conducted with three FO membranes and with increasing TMP up to a maximum of 50 psi (3.45 bar). The feed solution was a mixture of salts and the draw solution was either a NaCl solution or concentrated seawater at similar osmotic pressure. Results revealed that TMP minimally affected water flux, reverse salt flux (RSF), and solute rejection of the CTA membrane. However, water flux through TFC membranes might slightly increase with increasing TMP, and RSF substantially declines with increasing TMP. It was observed that rejection of feed constituents was influenced by TMP and RSF.

1. INTRODUCTION

Since the first academic review on the principles and applications of forward osmosis (FO), more than 150 journal articles have been published focusing on new developments and advancements made in both industry and academia.² The process has successfully established itself as a robust treatment technology capable of meeting the needs of various water and wastewater treatment applications such as management of landfill leachates, ^{1,3} concentrating of liquid foodstuff and beverages, ⁴⁻⁷ treatment of domestic wastewaters, ⁸⁻¹¹ concentration of anaerobic digester centrate, ¹² and more recently treatment of oil and gas exploration and production wastewater. 13 The continuous pursuit of advanced industrial wastewater treatment technologies has spurred academic and industrial research to develop better performing FO membranes; increasing water permeability and membrane robustness while maintaining high contaminant rejection, and minimizing solute reverse transport through the membranes. 14-16 These rapid progressions, both in industrial applications and academic research and development, require not only standardized membrane testing methods, but also development of advanced testing apparatuses and procedures to simulate true industrial conditions at the bench scale.

A joint effort by seven laboratories recently resulted in standard testing protocols under which FO membrane performance can be evaluated and compared, addressing the lack of uniform testing methods used in previous studies. 17,18 The study suggested several operating conditions that should be held constant when assessing the performance and integrity of FO membranes. These include hydraulic transmembrane pressure (TMP), system temperature, draw solution (DS) solute and concentration, and cross-flow velocity. This method provides an unbiased platform for comparison of new and commercially available FO membranes. However, it is not clear if membrane performance under these standardized laboratory conditions can be compared to those experienced in industrial scenarios.

The net transport of water across membranes in FO is driven by a difference in osmotic pressure and intrinsically requires no hydraulic TMP, which should be minimized (e.g., close to 0 psi) under standard laboratory conditions. Conversely, industrial FO applications require pressurization of the feed and DS streams to overcome hydraulic resistance in the flow channels of spiral or capillary wound membrane modules. When several elements are connected in series, adequate hydraulic pressure must be supplied at the entrance (leading element) to ensure feed and DS flow through the entire vessel and residual pressure at the last element (tail element). This can translate into nearly 60 psi hydraulic pressure in the feed channels of the first FO element in a pressure vessel, resulting in net TMP if the pressure is different

Received: November 12, 2012 Revised: January 28, 2013 Accepted: January 30, 2013 Published: January 30, 2013



[†]Colorado School of Mines, Golden, Colorado, USA

^{*}New Mexico State University, Las Cruces, New Mexico, USA

between the feed and DS streams. In hollow fiber and plate-and-frame membrane modules, DS flow may be driven by vacuum to maintain membrane structural integrity. This too introduces hydraulic TMP across the membrane in addition to the osmotic driving force. Consequently, existing standard testing methods may not properly capture true membrane performance in the presence of hydraulic TMP.

The overall objective of this study was to investigate changes in membrane performance as a function of increasing hydraulic TMP. This study is not meant to supplement those methodologies previously published, 17 but to highlight the knowledge gap that still exists between standardized membrane comparisons at the bench scale and performance comparisons under hydraulic conditions common in industrial applications. TMP effects on FO membrane fouling were previously explored; however, they only supplemented a study on water recovery from sewage - it lacked a methodical experimental investigation and laboratory analyses. 11 The current study focuses on water flux, reverse salt flux (RSF), inorganic and organic feed ion rejection, and bidirectional solute flux, all of which have been thoroughly investigated in the past; 1,19-22 however, prior studies have not considered membrane performance under elevated TMPs. Three commercial membranes were tested and experimental conditions followed standardized methods whenever possible while still addressing the objectives of this study. It is important to note that TMP in this study (higher pressure in the feed stream) should not be confused with TMP in pressure-retarded osmosis (PRO) (higher pressure in the DS). A thorough study on the effects of TMP in PRO is provided elsewhere.²²

2. MATERIALS AND METHODS

2.1. Membrane Selection. Three flat sheet FO membranes were tested. The first membrane was an asymmetric cellulose triacetate (CTA) membrane from Hydration Technology Innovations (HTI) (Albany, OR). The other two membranes were thin film composite (TFC) polyamide-based membranes manufactured by Oasys (Boston, MA) (designated TFC1) and HTI (designated TFC2). Although commercial and partially tested in the field, both TFC membranes are still under development and experience varying performance under similar testing conditions. ^{24–26} The three membranes were tested with their active layer facing the feed solution. Physical and chemical membrane characteristics are summarized in Table S1 of the Supporting Information.

Membrane samples were stored at 5 °C and rinsed with Milli-Q deionized water prior to installation. TFC1 was also wetted in situ using a 50% isopropyl alcohol solution for 5 min following manufacturer recommendations to ensure complete pore saturation (Table S1). To ensure unbiased results (i.e., water flux and RSF), integrity tests with 1 M NaCl DS and Milli-Q water feed were performed after installation of a new membrane and after every two experiments with inorganic feed solution. The membranes were replaced if the water flux or RSF differed by more than 10% from the initial integrity test. Integrity tests were performed during experiments with humic acid in the feed stream, but the membrane was replaced after each experiment due to potential organic fouling of the membrane.

2.2. Membrane Characterization. Water permeability coefficients (A), solute (NaCl) permeability coefficients (B), and membrane structural parameters (S), were determined through RO and FO tests. ¹⁷ A cross-flow test cell with a membrane area of 42 cm² was used with fixed feed flow velocity of 25 cm/s, constant feed temperature of 20 ± 0.5 °C, and feed

volume of 20 L. Experiments were conducted with either deionized water or 35 mM NaCl feed solution. The cumulative weight of permeate was continuously measured with an analytical balance connected to a data acquisition system (Lab VIEW, National Instruments (Austin, TX) and UE9-Pro, LabJack (Lakewood, CO)). The conductivity of the feed and permeate streams was continuously measured using calibrated conductivity probes (Oakton Instruments, Vernon Hills, IL). The values were logged into the data acquisition system that continuously calculated water flux and solute rejection.

Before RO tests, membranes were compacted with deionized water feed at 125 psi until steady state water flux was reached. Low compaction pressures were used due to the highly permeable nature of the chosen membranes. Pure water flux was then measured at feed pressures of 50, 100, and 125 psi for three hours each. This procedure was repeated with a 35 mM NaCl feed solution. Experimental results from RO tests were used to calculate A and B, and the experimental results from FO tests with deionized feedwater and 1 M NaCl DS were used to calculate S, as described in previous publications. 17,27,28

The surface charge of each membrane's active and support layer was determined by zeta-potential measurement using an electrokinetic analyzer (SurPass, Anton Paar GmbH, Austria) using a 2 mM KCl electrolyte solution. The hydrophobicity of the membrane active layer was determined using sessile drop (TFC1 and TFC2) and captive bubble (CTA) contact angle measurements and deionized water.

2.3. Bench-Scale FO System. The bench-scale FO apparatus used was similar to that described in a previous publication¹⁷ (Figure S1 of the Supporting Information). A custom membrane test cell consisting of symmetric flow channels $(26.35 \times 5.50 \times 0.17 \text{ cm})$ and 145 cm^2 effective area was utilized. Nitrile rubber gaskets provided membrane support and adequate depth in each flow channel. Commercially available turbulence-enhancement net and tricot spacers were installed in the DS flow channel to provide membrane support under a hydraulically pressurized feed. The tricot spacer was in contact with the membrane support layer mimicking the conditions inside a spiral wound membrane element. Data acquisition software was utilized to control experimental conditions (i.e., system temperature of 20 ± 0.5 °C, feed solution volume of 3 L, and DS concentration) and to collect experimental data (i.e., feed and DS conductivities, feed solution volume). Feed and draw solutions were circulated cocurrently in the test cell at 25 cm/s and returned to their respective tanks. Further details on system design and operation are available elsewhere. 20,29

2.4. Solution Chemistry. *2.4.1. Draw Solutions.* ACS grade NaCl (Fisher Scientific, Fair Lawn, NJ) was used to prepare the DS. Stock solution was prepared in 20 L batches to eliminate variability in DS chemistry. During experiments with inorganic feed solution, the concentration of DS was maintained at 1 M by dosing a concentrated stock solution of 300 g/L NaCl (ACS, Sigma-Aldrich, St. Luis, MO). During experiments using organic feed solution, the DS was osmotically diluted.

Formulated sea salt (Instant Ocean, Madison, WI) was used to prepare surrogate seawater DS for specific sets of experiments (composition provided in Table S2 of the Supporting Information). The seawater DS was prepared in 20 L batches at a concentration of 60.1 g/L to generate osmotic pressure similar to the 1 M NaCl DS (approximately 680 psi (47 bar)). The seawater DS concentration during FO experiments was maintained constant by slow dosing of a concentrated sea salt (175 g/L).

2.4.2. Inorganic Feed Solution. Three ACS grade inorganic salts were used for the preparation of the feed solution. These include MgSO₄, KNO₃, and LiBr (Fisher Scientific, Fair Lawn, NJ). Stock solution containing 20 mM of each salt was mixed with Milli-Q water in 20 L batches. The calculated osmotic pressure of the feed solution was 36 psi (2.5 bar). These salts were chosen to investigate the effects of TMP and solute properties such as molecular weight and ionic and hydration radius on solute rejection and RSF. Distilled water (Corning, Mega-Pure MP-3A) was used to replenish the 3 L feed volume (compensating for water that permeated through the FO membrane into the DS) in order to minimize ion loading into the feedwater.

2.4.3. Organic Feed Solution. A composite organic feed solution of ACS grade humic acid and NaCl (Sigma-Aldrich, St. Louis, MO) was tested in a separate set of experiments. A concentrated stock solution of 5 g/L humic acid was prepared using Milli-Q water. Twenty liter batches of feed solution were prepared with 10 mM NaCl in Milli-Q water. For each experiment 3 L of the NaCl feed solution was transferred into the feed tank. Subsequently, 30 mL feed solution was removed from the feed tank and replaced with 30 mL humic acid stock solution. The resulting humic acid concentration in the feed solution was 50 mg/L.

2.5. Experimental Procedures. *2.5.1. Experiments with Inorganic Feed Solution.* A set of five tests was conducted with each membrane using inorganic feed solution and NaCl DS. With the membrane test cell removed, 3 L of feed solution and 1 L of DS were transferred to their respective tanks and brought to constant temperature. Subsequently, the test cell was connected horizontally with feed solution flowing on top and DS flowing under the membrane.

A baseline experiment was first conducted under true FO conditions (e.g., $\Delta P = 0$ psi). The TMP was then increased and held constant in each successive test in favor of the feed; thus, TMPs of 6, 18, 30, and 50 psi were investigated in each set of experiments. This pressure differential was maintained using needle valves installed on the test cell discharge lines with higher pressure in the feed stream (Figure S1 of the Supporting Information). Feed and DS pressures were monitored using pressure gauges (Ashcroft, Stratford, CT) installed at the test cell inlets. The feed volume and the DS concentration were held constant throughout each experiment. These conditions sustained a constant osmotic driving force, allowing for an unbiased comparison of water flux and ion transport between experiments with different TMP. RSF was monitored using a calibrated conductivity probe installed in the feed tank (Oakton Instruments, Vernon Hills, IL) and verified analytically using IC and ICP analysis of feed samples. Water flux was calculated using the change of weight of deionized water in the feed dosing tank positioned on the analytical balance.

A set of three additional tests was conducted on each membrane using seawater DS. Experimental setup and preparation followed the same procedure; however, after initial baseline experiments ($\Delta P = 0$ psi), only two additional tests were conducted, one at 6 psi and the other at 18 psi TMP.

2.5.2. Experiments with Organic Feed Solution. A set of two tests (TMP = 0 or 18 psi) was conducted on each membrane using organic feed solution and NaCl DS. Experimental preparation and data collection followed procedures described in the previous section; however, tests were conducted under osmotic dilution mode in which the DS was slowly diluted as water permeated through the FO membrane. Feed volume was

held constant by replenishing the feed reservoir with distilled water. We operated in osmotic dilution mode because the concentrated NaCl dosing solution contained TOC impurities that under regular FO operation will make it impossible to quantify TOC transport from the feed into the DS.

2.6. Sampling and Analytical Methods. Six samples were drawn during each experiment with inorganic feed solution. Feed and DS baseline samples were taken from each tank after 15 min from the beginning of each experiment and after 750 and 1500 mL of water permeated through the membrane into the DS. The change in individual ion concentrations was measured and correlated to the volume of each tank at the time of sampling. Therefore, the change in mass of each ion could be calculated in both solutions to determine its flux and direction of diffusion. To ensure accurate mass balance calculations, samples were also drawn from the feed and DS dosing tanks to correct for ions dosed to each tank that did not diffuse through the membrane. Samples were stored at 5 °C prior to dilution for analysis.

Cation and anion concentrations were analyzed for each sample using inductively coupled plasma atomic emission spectroscopy (ICP-AES) (Optima 5300, PerkinElmer, Fremont, CA) and ion chromatography (IC) (ICS-90, Dionex, Sunnyvale, CA), respectively. Cations were tested in triplicates with a maximum allowable deviation of 10% and anions in duplicates with a maximum allowable deviation of 5%. Analytical results were used to calculate the mass balance of individual ions to assess the effects of TMP on forward and reverse solute transport.

Four samples were drawn during each experiment with organic feed solution. Baseline samples from the feed and DS tanks were taken after 15 min from the beginning of each experiment and after 2000 mL of water permeated through the membrane into the DS. Similar mass balance calculations to those using inorganic feed solution were conducted. Samples were preserved using concentrated phosphoric acid and stored at 5 °C prior to dilution for analysis in triplicates using a carbon analyzer (Shimadzu TOC-L, Columbia, MD).

3. RESULTS AND DISCUSSION

3.1. Water Flux. Water flux was calculated after each FO experiment to determine the effects of applied hydraulic TMP on water permeability through the membrane. Water flux as a function of TMP is shown in Figure 1 for experiments conducted with inorganic feed solution and NaCl or seawater DS.

Minimal changes in water flux were observed for the three membranes when TMP was elevated. The small fluctuations in flux are within the range of experimental errors associated with the tested membranes. Water flux through TFC1 fluctuated but, considering the high flux through this membrane, the changes were minimal. This membrane also showed high flux variability in previous studies. Water flux through the CTA membrane was relatively constant, regardless of the DS used, and flux through TFC2 constantly increased when subjected to rising TMP, both with NaCl and seawater DSs. It is likely that TFC2 has some characteristics of loose RO and NF membrane, which affect both water flux and salt rejection through this membrane. It is worth noting that results from preliminary tests revealed that membrane compaction had negligible effects on water flux through the three membranes.

Water flux through the TFC membranes at 0 psi TMP during experiments with both the NaCl DS (part a of Figure 1) and seawater DS (part b of Figure 1) was lower than those measured during integrity tests (Table S1 of the Supporting Information).

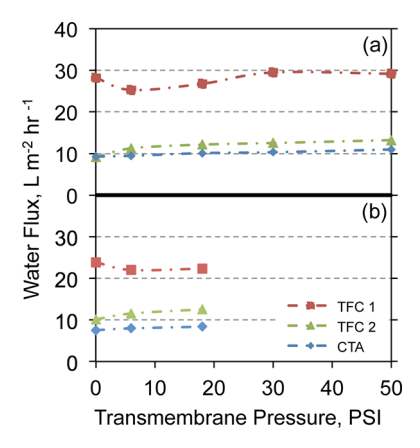


Figure 1. Water flux as a function of TMP for (a) experiments with 1 M NaCl DS and (b) 60.1 g/L seawater DS. Both DSs were maintained at constant concentration and the feed solution volume was held constant. The system was maintained at 20 \pm 0.5 °C. Feed was a solution of MgSO₄, KNO₃, and LiBr, 20 mM each.

This is attributed to the elevated salinity of the feed in the current experiments coupled with increased concentration polarization expected with high flux. A more pronounced decrease in water flux was observed with seawater DS. Whereas the calculated osmotic pressure of the two DSs was similar, larger ions such as magnesium, calcium, sulfate, and carbonates induce lower flux in FO compared to smaller ions such as sodium, chloride, and potassium.²⁰

3.2. Reverse Salt Flux. RSF was measured by both monitoring increasing feed conductivity during the experiments and through IC and ICP-AES analysis of feed and DS samples. RSF as a function of TMP is shown in Figure 2 for experiments conducted with NaCl or seawater DSs.

When increasing the TMP, very little change in RSF through the CTA membrane was observed during all experiments. Different trends were observed for TFC1 and TFC2, where increased TMP resulted in a decline of RSF. During both NaCl DS experiments (parts a and b of Figure 2) and seawater DS

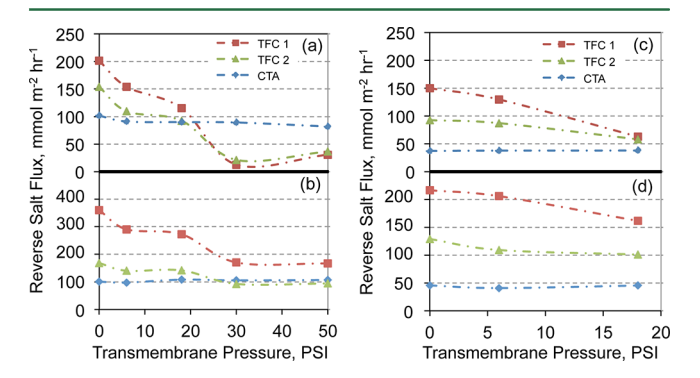


Figure 2. RSF (NaCl) measured in the feed solution as a function of TMP with (a) a calibrated conductivity probe in the feed reservoir (1 M NaCl DS), (b) IC and ICP-AES analysis of feed samples (1 M NaCl DS), (c) a calibrated conductivity probe in the feed reservoir (60.1 g/L seawater DS), and (d) IC and ICP-AES analysis of feed samples (60.1 g/L SW DS). RSF from IC and ICP-AES data was calculated based on the slower reverse diffusing ion through the membrane (sodium for the CTA membrane and chloride for the TFC membranes) assuming that the difference in ion flux is due to balancing effects of forward diffusing ions. All experiments were conducted with inorganic feed solution at 20 \pm 0.5 °C. For seawater DS, IC and ICP-AES results (c and d) reflect transport of sodium and chloride only.

experiments (parts c and d of Figure 2), a decline in RSF was observed when TMP increased from 0 to 50 psi. The decline in RSF may be attributed to physical changes in the membrane active layer as a function of the hydraulic pressure. Increasing pressure at the membrane surface may have compressed the interface between the thin active layer and support layer of the TFC membranes, thus reducing RSF and salt permeability of the membrane, while minimally affecting water flux.

Data presented in Figure 2 also highlights several important topics when addressing RSF through FO membranes, especially TFC membranes. Results in parts a and c of Figure 2 show different RSF values than those calculated using results from IC and ICP-AES analysis (parts b and d of Figure 2). These results indicate dissimilar RSF because the use of a conductivity probe does not distinguish between the diffusion of NaCl into the feed solution and solutes leaving the feed solution, nor do these probes account for different rates of reverse diffusion of individual ions. Specifically, RSF values that rely on the use of conductivity measurements (e.g., field analysis and pilot studies) cannot capture the different rates of bidirectional diffusion of solutes from the feed into the DS and vice versa. Whereas trends are similar in both analytical methods, different RSF values can be expected when calculated using IC and ICP-AES results because it only accounts for the reverse diffusion of sodium and chloride. Furthermore, comparison of membrane performances can also be impacted as shown in parts a and b of Figure 2, where TFC1 RSF declines below that of CTA when analyzed with a conductivity probe but is not true when using IC and ICP-AES results to calculate RSF.

Another interesting trend in RSF through the TFC membranes at 0 psi TMP for both DSs (Figure 2) should be noted, where RSF was lower than that measured during integrity tests (Table S1 of the Supporting Information). Similar to water flux through TFC1 at 0 psi TMP, the lower RSF is attributed to the elevated salinity of the feed in the current experiments coupled with increased concentration polarization expected with high water flux. Results from IC and ICP analysis and from conductivity probe measurements used for determining RSF during experiments with inorganic feed solution cannot be used for direct comparison to RSF during integrity tests with DI water feed. This is because the reverse flux of sodium and chloride are different and affected by forward diffusing feed ions and concentration polarization.

3.3. Feed Ion Rejection. The rejection of feed ions and the reverse diffusion of individual DS solutes into the feed solution were measured concurrently with water flux (Figure 1) and RSF (Figure 2). Percent rejection of feed ions and reverse flux of DS ions are shown in Figure 3 for a range of TMPs for the three membranes investigated. Feed ion rejection was calculated only for results from experiments with NaCl DS and inorganic feed solution. This minimized the effects of bidirectional solute diffusion of minor ions in seawater that will make mass balance calculation very difficult (for common feed and DS ions).

Based on minimal changes in RSF observed in parts a and b of Figure 2, CTA rejection of feed ions was expected to remain constant with increasing TMP. Results in part a of Figure 3 reveal that indeed little changes in anion or cation rejection were observed when TMP increased. Percent rejection of individual ions was as expected, with ions of decreasing size and hydration radius diffusing more readily from the feed into the DS. ³⁰ RSF of NaCl was decoupled into reverse fluxes of sodium and chloride in an attempt to explain why cation rejection was greater throughout CTA experiments. It can be seen in part b of Figure

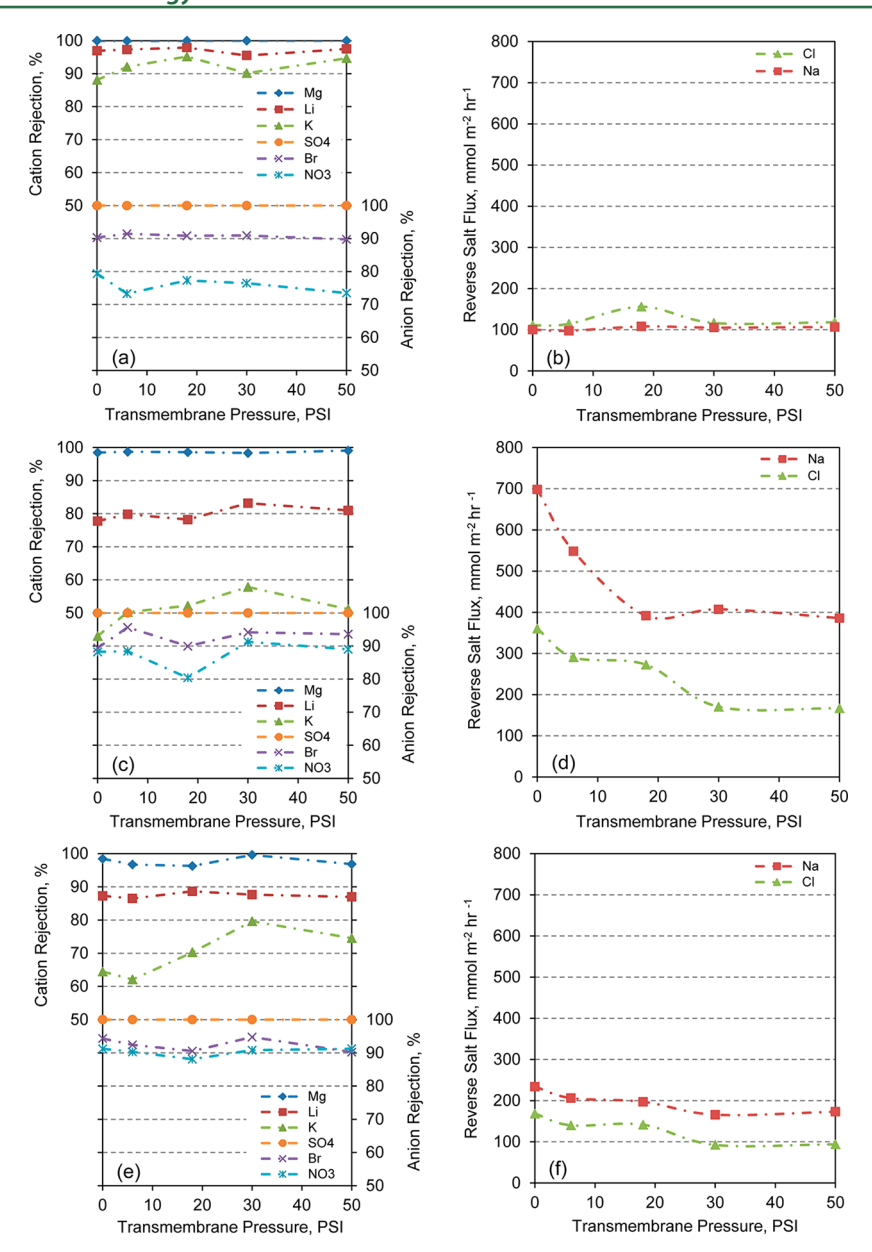


Figure 3. Ion rejection as a function of TMP for (a) CTA, (c) TFC1, and (e) TFC2. The reverse flux of sodium and chloride for each data set presented is also provided for (b) CTA, (d) TFC1, and (f) TFC2. Experiments were conducted using 1 M NaCl DS and inorganic feed solution at 20 ± 0.5 °C. Draw solution concentration and feed solution volume were held constant throughout all experiments.

3 that the reverse flux of chloride was nearly double that of sodium throughout all experiments. Consequently, lower anion rejection was observed as anions more readily diffused into the DS to maintain electroneutrality.

The order of ion rejection by the TFC1 and TFC2 membranes was similar to that by the CTA membrane — ions with a smaller hydration radius diffused more readily into the DS, and DS ions diffused accordingly to maintain system electroneutrality. Data presented in parts a and b of Figure 2 suggests that ion rejection should increase with increasing TMP for both TFC membranes due to observed decrease in RSF; this hypothesis is supported by results in parts c and e of Figures 3. Contrary to the results observed with the CTA membrane, reverse flux of sodium was higher than that of chloride throughout all tests with the TFC membranes. Consequently, observed cation rejection was lower than anion rejection because positive ions diffused faster into the DS to balance higher sodium reverse diffusion from the DS into

the feed. During experiments with TFC1 potassium and lithium rejection increased by approximately 7% and 3%, respectively, between 0 and 50 psi TMP, whereas nitrate and bromide rejection increased by approximately 1% and 5%, respectively. Magnesium and sulfate were nearly completely rejected during all experiments, which is expected due to their large molecular size. During experiments with TFC2 potassium rejection increased by approximately 10% between 0 and 50 psi TMP, while lithium rejection remained unchanged. Sulfate was completely rejected, similarly to TFC1, whereas magnesium rejection was slightly lower than expected (~96%). Low magnesium rejection by TFC2 may be attributed to the slight decline observed in nitrate and bromide rejection in order to maintain solution electroneutrality.

In all cases, nitrate rejection was the lowest of all anion species that were monitored. These results are similar to those observed for nitrate in previous FO studies 12,21,31 and for results in

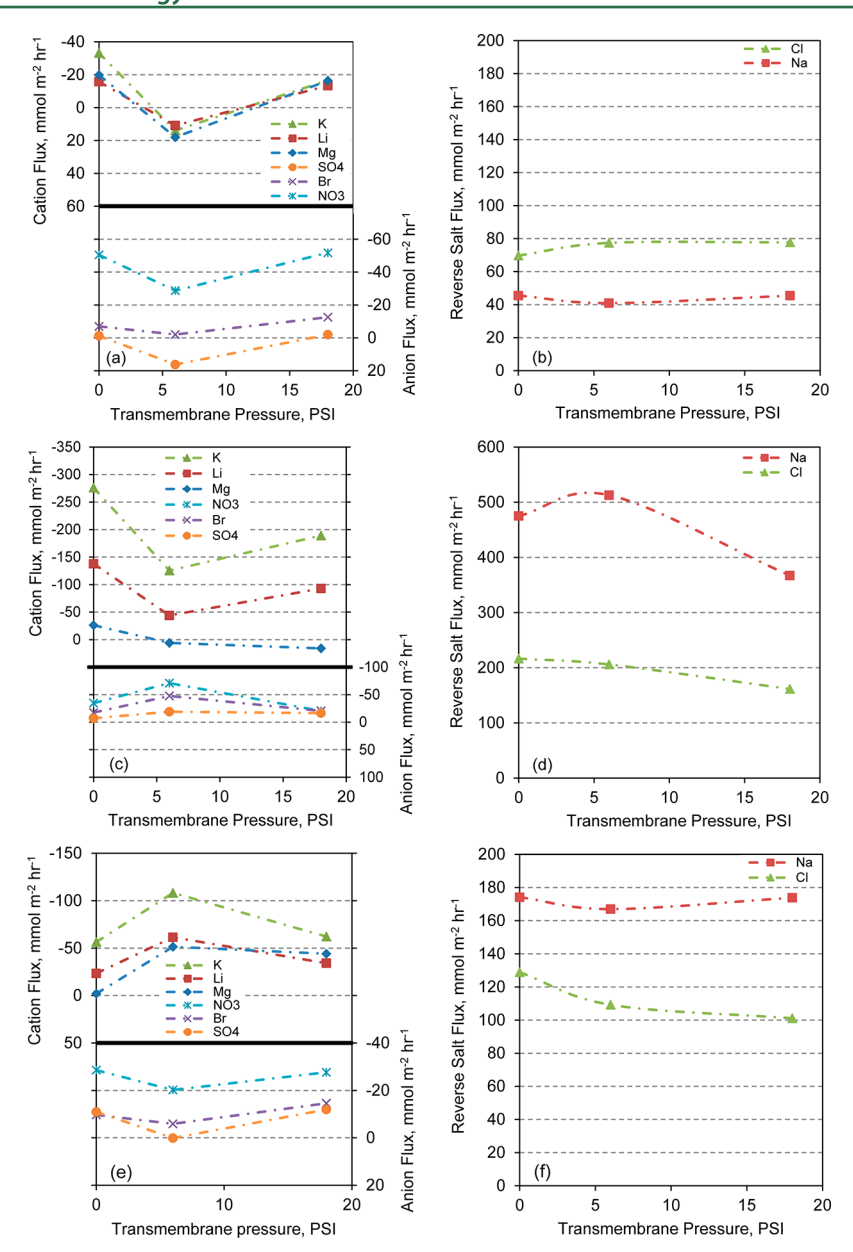


Figure 4. Inorganic ion mass flux as a function of TMP for (a) CTA, (c) TFC1, and (e) TFC2. Negative ion flux represents solute diffusion from the feed into the DS. The reverse flux of sodium and chloride (from seawater) as a function of TMP for each data set presented is also provided for (b) CTA, (d) TFC1, and (f) TFC2. Experiments were conducted using 60.1 g/L sea salt DS and inorganic feed solution at 20 ± 0.5 °C. DS concentration and feed solution volume were held constant throughout all experiments. The average charge imbalance was 8.5%, 9.2%, and 9.4% for solutions analyzed during CTA, TFC1, and TFC2 experiments, respectively. The average ion flux imbalance measured in meq m⁻² hr⁻¹ was 14.4%, 3.1%, and 15.5% for solution mass balance calculations analyzed for CTA, TFC1, and TFC2 experiments, respectively.

nanofiltration studies. Substantially higher rate of sodium reverse diffusion through the TFC membranes is attributed to the significantly low negative charge of their support layer (-9.5 to -3 mV vs -40 mV for the CTA) and therefore higher electrostatic attraction of sodium to the back side of the polyamide active layer of the TFC membranes.

3.4. Bidirectional Solute Flux. Bidirectional solute flux was quantified using data from experiments with seawater DS and inorganic feed solution. It was expected that by introducing feed ions into the DS in ratios found in sea salt, the rates of reverse and forward diffusion of some ions will be different than those presented in Figure 3. Ionic mass balance was calculated using IC and ICP-AES data and results are shown in Figure 4 as mass flux for both feed ions (all) and DS ions (sodium and chloride only).

Data in parts a, c, and e of Figure 4 also captures ions that diffuse from the seawater DS into the feed.

RSF through the CTA membrane remained fairly constant across all pressures with chloride diffusion exceeding that of sodium (part b of Figure 4). Higher diffusion of nitrate ions from the feed into the DS was observed to maintain charge neutrality with reverse diffusion of chloride into the feed. The remaining major feed cations and anions diffused in both directions across the membrane with no apparent correlation to increased TMP; this lack of correlation to TMP was expected given relatively steady RSF in part b of Figure 4 and data presented in parts a and b of Figure 3. The average feed solution charge imbalance and feed ion flux imbalance, measured in meq·m⁻²·hr⁻¹, was 8.5% and 14.4%, respectively.

Similar to early results, RSF through the TFC1 membrane (part d of Figure 4) showed a decreasing trend with higher observed reverse diffusion of sodium than that of chloride. Once again, forward diffusion of cations from the feed to the DS was higher than that of anions (part c of Figure 4) to account for greater reverse diffusion of sodium. The average feed solution charge imbalance and feed ion flux imbalance was 9.2% and 3.1% respectively and within the accuracy range of the analytical instruments. RSF through the TFC2 membrane (part f of Figure 4) once again decreased with increasing TMP; however, at a much lower rate than that observed in part f of Figure 3. The membrane coupons used during testing with seawater DS may have a relatively denser active layer as suggested by the lower observed RSF in Table S1 of the Supporting Information. Similar ionic diffusion behavior to that of TFC1 was observed while maintaining an average feed solution charge imbalance and ion flux imbalance of 9.4% and 15.5%, respectively.

Overall, it is very difficult to conduct an accurate mass balance with complex feed and DSs that have similar constituents on both sides of the membrane. Similar to results with NaCl DS and previous studies, nitrate diffusion through all FO membranes is faster, and its rejection is lower than other anions regardless of feed pressure and DS used. Most interestingly, in both the NaCl and the concentrated seawater DS experiments, reverse diffusion of sodium was higher through the TFC membranes and lower through the CTA membrane. The more negatively charged support layer of TFC2 compared to TFC1 reduced the electrostatic attraction of sodium to the active layer (through the support layer) and resulted in higher reverse diffusion of sodium through TFC1. Furthermore, TFC1 is a much more permeable membrane and allows more free transport of ions through the membrane. This phenomenon might be related to the different surface charge on the support sides of the TFC membranes (Table S1 of the Supporting Information) and should be further explored.

3.5. Rejection of Humic Acids. Rejection of organic molecules was evaluated through mass balance calculations using data from carbon analysis of feed and DS samples. Percent rejection of TOC as a function of TMP at 0 and 18 psi is summarized in Table 1 for the three membranes investigated in

Table 1. TOC Rejection As a Function of TMP for the Three Membranes Tested in the Study

	TOC Rejection (%)	
membranes	0 PSI	18 PSI
CTA	96.2 ± 0.6	95.3 ± 0.1
TFC1	95.6 ± 0.5	92.4 ± 0.3
TFC2	96.0 ± 0.1	96.2 ± 0.2

this study. Humic acid was not purified prior to injection into the feed solution to more closely mimic organic matter in natural systems; the TOC content of the humic acid used in this study was approximately 38%.

Minimal changes in TOC rejection were observed when TMP increased from 0 to 18 psi, and the three membranes showed similar rejection of organic molecules. Comparable rejection suggests that a large fraction of the chosen humic acid has high molecular weight molecules that are well rejected by the active layers of the CTA and TFC membranes. A small fraction of low molecular weight organics is likely present and readily diffuses through the membranes. TFC1 is the most delicate membrane among the three (very thin active and support layers) and

therefore it is likely that higher pressure in conjunction with membrane installation associated with bench scale systems resulted in a slightly lower organic rejection by TFC1 at higher pressures. It is also likely that the lower organic rejection of TFC1 is attributed to slight differences in membrane integrity between the membrane coupons used in the first and second sets of FO tests.

The specific water flux (water flux normalized by the net driving force, which is also the instantaneous membrane permeability coefficient) was calculated for each test conducted during this investigation. Because the experiments were conducted in osmotic dilution mode, the osmotic pressure driving force slowly declined and it was necessary to take into consideration internal concentration polarization effects in order to calculate the instantaneous water permeability coefficients. The feed and DS osmotic pressures were calculated using OLI Analyzer Studio (OLI Systems, Inc., Morris Plains, NJ) and used to determine the effective osmotic pressure driving force as a function of time in each test. Results (not shown) revealed that the water permeability coefficient of the three membranes have not changed during the course of the experiments, indicating that membrane fouling was negligible during the experiments.

Results from this study show that new standard testing methods of FO may provide a good platform for comparative membrane testing in the laboratory; however, they do not capture accurately membrane performance when operated under higher TMP typical in industrial applications. Introduction of hydraulic pressure across the membrane can result in changes of membrane performance compared to baseline performance under FO conditions in which TMP is 0 psi.

CTA membranes showed little changes in membrane performance as a function of increasing TMP. Results from standardized methods can be assumed accurate up to the maximum pressure tested in this study. Conversely, increasing TMP did impact the performance of TFC membranes; however, these changes are not necessarily an indication of poorer performance. Declining RSF was observed in both TFC membranes with some increase in water flux seen in TFC2. Such changes can impact the bidirectional diffusion of ions across the membrane and have significant impacts in industrial applications.

Results demonstrated that membrane material and structure, coupled with operating conditions, might influence the preferential forward and reverse diffusion of charged ions. This phenomenon is important and can impact specific process applications and requires further investigation. To ensure proper selection and applicability of FO membranes in specific industrial processes, the effects of hydraulic feed pressures and membrane material on water flux and ion transport should also be taken into consideration when conducting standard membrane comparisons.

ASSOCIATED CONTENT

Supporting Information

Details are available on FO membrane properties, rejection calculations, system configuration, and seawater quality. This material is available free of charge via the Internet at http://pubs.acs.org.

AUTHOR INFORMATION

Corresponding Author

*Tel.: +1 303 273 3402, fax: +1 303 273 3413, e-mail: tcath@mines.edu.

Notes

The authors declare no competing financial interest.

ACKNOWLEDGMENTS

Support of this investigation was provided by DOE/RPSEA project 10122-39. The authors would like to thank Hydration Technology Innovations and Oasys Water for providing membranes for the study. The authors would also like to thank Thomas Gately and Amanda Erskine for their assistance with water analyses.

REFERENCES

- (1) Cath, T. Y.; Childress, A. E.; Elimelech, M. Forward osmosis: Principles, applications, and recent developments. *J. Membr. Sci.* **2006**, 281 (1–2), 70–87.
- (2) Zhao, S.; Zou, L.; Tang, C. Y.; Mulcahy, D. Recent developments in forward osmosis: Opportunities and challenges. *J. Membr. Sci.* **2012**, 396, 1–21.
- (3) York, R. J.; Thiel, R. S.; Beaudry, E. G. In Full-scale experience of direct osmosis concentration applied to leachate management, Sardinia '99 Seventh International Waste Management and Landfill Symposium, S. Margherita di Pula, Cagliari, Sardinia, Italy, 4—8 October 1999, 1999; S. Margherita di Pula, Cagliari, Sardinia, Italy, 1999.
- (4) Jiao, B.; Cassano, A.; Drioli, E. Recent advances on membrane processes for the concentration of fruit juices: A review. *J. Food Eng.* **2004**, *63* (3), 303–324.
- (5) Petrotos, K. B.; Lazarides, H. N. Osmotic concentration of liquid foods. *Journal of Food Engineering* **2001**, 49, 201–206.
- (6) Petrotos, K. B.; Quantick, P.; Petropakis, H. A study of the direct osmotic concentration of tomato juice in tubular membrane module configuration. I. The effect of certain basic process parameters on the process performance. *J. Membr. Sci.* **1998**, *150* (1), 99–110.
- (7) Petrotos, K. B.; Quantick, P. C.; Petropakis, H. Direct osmotic concentration of tomato juice in tubular membrane module configuration. II. The effect of using clarified tomato juice on the process performance. *J. Membr. Sci.* 1999, 160 (2), 171–177.
- (8) Achilli, A.; Cath, T. Y.; Marchand, E. A.; Childress, A. E. The forward osmosis membrane bioreactor: A low fouling alternative to MBR processes. *Desalination* **2009**, 239 (1–3), 10–21.
- (9) Alturki, A.; McDonald, J.; Khan, S. J.; Hai, F. I.; Price, W. E.; Nghiem, L. D. Performance of a novel osmotic membrane bioreactor (OMBR) system: Flux stability and removal of trace organics. *Bioresour. Technol.* **2012**, *113*, 201–206.
- (10) Zhang, J.; Loong, W. L. C.; Chou, S.; Tang, C.; Wang, R.; Fane, A. G. Membrane biofouling and scaling in forward osmosis membrane bioreactor. *J. Membr. Sci.* **2012**, *403*–*404*, 8–14.
- (11) Lutchmiah, K.; Cornelissen, E. R.; Harmsen, D. J.; Post, J. W.; Lampi, K.; Ramaekers, H.; Rietveld, L. C.; Roest, K. Water recovery from sewage using forward osmosis. *Water Sci. Technol.* **2011**, *64* (7), 1443–1449.
- (12) Holloway, R. W.; Childress, A. E.; Dennett, K. E.; Cath, T. Y. Forward osmosis for concentration of anaerobic digester centrate. *Water Res.* **2007**, *41* (17), 4005–4014.
- (13) Hickenbottom, K. L.; Hancock, N. T.; Hutchings, N. R.; Appleton, E. W.; Beaudry, E. G.; Xu, P.; Cath, T. Y., Forward osmosis treatment of drilling mud and fracturing wastewater from oil and gas operations. *Desalination* **2012**, *in press*, doi:10.1016/j.desal.2012.05.037.
- (14) Qiu, C.; Setiawan, L.; Wang, R.; Tang, C. Y.; Fane, A. G. High performance flat sheet forward osmosis membrane with an NF-like selective layer on a woven fabric embedded substrate. *Desalination* **2012**, 287, 266–270.
- (15) Setiawan, L.; Wang, R.; Li, K.; Fane, A. G. Fabrication and characterization of forward osmosis hollow fiber membranes with antifouling NF-like selective layer. *J. Membr. Sci.* **2012**, 394–395, 80–88.
- (16) Wang, R.; Shi, L.; Tang, C. Y.; Chou, S.; Qiu, C.; Fane, A. G. Characterization of novel forward osmosis hollow fiber membranes. *J. Membr. Sci.* **2010**, 355 (1–2), 158–167.

- (17) Cath, T. Y.; Elimelech, M.; McCutcheon, J. R.; McGinnis, R. L.; Achilli, A.; Anastasio, D.; Brady, A. R.; Childress, A. E.; Farr, I. V.; Hancock, N. T.; Lampi, J.; Nghiem, L. D.; Xie, M.; Yip, N. Y., Standard methodology for evaluating membrane performance in osmotically driven membrane processes. *Desalination* **2012**, *in press*, doi:10.1016/j.desal.2012.07.005.
- (18) Wang, K. Y.; Ong, R. C.; Chung, T.-S. Double-skinned forward osmosis membranes for reducing internal concentration polarization within the porous sublayer. *Ind. Eng. Chem. Res.* **2010**, 49 (10), 4824–4831.
- (19) Achilli, A.; Cath, T. Y.; Childress, A. E. Selection of inorganic-based draw solutions for forward osmosis applications. *J. Membr. Sci.* **2010**, *364* (1–2), 233–241.
- (20) Hancock, N. T.; Cath, T. Y. Solute coupled diffusion in osmotically driven membrane processes. *Environ. Sci. Technol.* **2009**, 43 (17), 6769–6775.
- (21) Hancock, N. T.; Phillip, W. A.; Elimelech, M.; Cath, T. Y. Bidirectional permeation of electrolytes in osmotically driven membrane processes. *Environ. Sci. Technol.* **2011**, 45 (24), 10642–10651.
- (22) Phillip, W. A.; Yong, J. S.; Elimelech, M. Reverse draw solute permeation in forward osmosis: modeling and experiments. *Environ. Sci. Technol.* **2010**, *44*, 5170–5176.
- (23) She, Q.; Jin, X.; Tang, C. Y. Osmotic power production from salinity gradient resource by pressure retarded osmosis: Effects of operating conditions and reverse solute diffusion. *J. Membr. Sci.* **2012**, 401–402, 262–273.
- (24) HTI's new thin film forward osmosis membrane in production. http://www.htiwater.com/news/press-room/content/2012/press-HTI-HTIThinFilmMembrane042512.pdf
- (25) McGinnis, R. L.; Hancock, N. T.; Nowosielski-Slepowron, M. S.; McGurgan, G. D., Pilot demonstration of the NH3/CO2 forward osmosis desalination process on high salinity brines. *Desalination* **2013**, http://dx.doi.org/10.1016/j.desal.2012.11.032.
- (26) Oasys, FO process concentrates oilfield brine. http://oasyswater.com/blog/news/fo-process-concentrates-oilfield-brine/
- (27) Yip, N. Y.; Tiraferri, A.; Phillip, W. A.; Schiffman, J. D.; Elimelech, M. High performance thin-film composite forward osmosis membrane. *Environ. Sci. Technol.* **2010**, *44* (10), 3812–3818.
- (28) Tiraferri, A.; Yip, N. Y.; Phillip, W. A.; Schiffman, J. D.; Elimelech, M. Relating performance of thin-film composite forward osmosis membranes to support layer formation and structure. *J. Membr. Sci.* **2011**, 367 (1–2), 340–352.
- (29) Hancock, N. T. Engineered osmosis: Assessment of mass transport and sustainable hybrid system configurations for desalination and water reclamation. Colorado School of Mines, Golden, 2011.
- (30) Nightingale, E. R. Phenomenological theory of ion solvation. Effective radii of hydrated ions. *J. Phys. Chem.* **1959**, 63 (9), 1381–1387.
- (31) Hancock, N. T.; Cath, T. Y. Solute coupled diffusion in osmotically driven membrane processes. *Environ. Sci. Technol.* **2009**, 43, 6769–6775.
- (32) Bellona, C.; Drewes, J. E. The role of membrane surface charge and solute physico-chemical properties in the rejection of organic acids by NF membranes. *J. Membr. Sci.* **2005**, 249 (1–2), 227–234.
- (33) McCutcheon, J. R.; Elimelech, M. Modeling water flux in forward osmosis: implications for improved membrane design. *AIChE J.* **2007**, 53, 1736–1744.

■ NOTE ADDED AFTER ASAP PUBLICATION

Note Added after ASAP Publication. This article was published ASAP on February 13, 2013, with minor display errors in Figures 3 and 4. The corrected article was published on February 19, 2013.